

Reaction Enthalpies for $M^+L = M^+ + L$, Where $M^+ = Na^+$ and K^+ and $L =$ Acetamide, *N*-Methylacetamide, *N,N*-Dimethylacetamide, Glycine, and Glycylglycine, from Determinations of the Collision-Induced Dissociation Thresholds

John S. Klassen, Stephen G. Anderson, Arthur T. Blades, and Paul Kebarle*

Department of Chemistry, University of Alberta, Edmonton, Alberta, Canada T6G 2G2

Received: March 19, 1996; In Final Form: May 31, 1996[⊗]

With electrospray (ES), ions present in solution can be transferred to the gas phase. The method provides unique opportunities for studies of hitherto inaccessible ions. Collision-induced dissociation threshold measurements of gas phase ions produced by ES are described. The thresholds for the reactions $M^+L = M^+ + L$, where M^+ is Na^+ or K^+ and L is acetone, dimethyl sulfoxide, acetamide, *N*-methylacetamide, *N,N*-dimethylacetamide, glycine, glycylglycine, succinamide, and glycyglycine, were determined. Enthalpy changes for the reaction were derived from these data.

Introduction

The bond enthalpies corresponding to reaction 1, where M^+



= Na^+ , K^+ and $L = CH_3NHCOCH_3$, are of special interest because of attempts to understand the microscopic factors controlling the passage of these ions through transmembrane channels such as the gramicidin channel. The permeation of the ion through the channel involves partial dehydration of the ion, where the endoergicity of the dehydration is offset by attractive interactions of the ion with polar groups in the channel.¹ The ion–channel interactions are believed to involve mainly the carbonyl oxygens of the peptide backbone.^{2–4}

Theoretical investigations of the Monte Carlo and molecular dynamics techniques rely on the development of realistic pair potential functions representing the microscopic interactions. For ion–solvent molecule interactions, such as ion–water molecule interactions, the pair potential functions were developed on the basis of ab initio calculations of the ion–molecule interactions.⁵ Of considerable help to this approach were the experimentally determined free energy, ΔG°_1 , enthalpy, ΔH°_1 and entropy, ΔS°_1 changes obtained from ion–solvent molecule equilibria observed by mass spectrometric techniques.⁶ These experimental data helped establish the quality of the basis set and electron correlation required in order to obtain values⁵ in agreement with experiment.

The interactions of the ions with peptides such as the transmembrane channels are also amenable to this approach, but in this case, rather than the actual peptide, a model compound such as methylacetamide is used to obtain information on the dominant interactions.⁷ Previous experimental ion–equilibria determinations are available only for K^+ and dimethylacetamide.⁸ It is therefore desirable to extend the equilibria determinations, which lead to the bond enthalpy and free energy changes ΔH°_1 and ΔG°_1 , to *N*-methylacetamide, acetamide and Na^+ ions.

The previous determinations⁸ were obtained with alkali ions produced in the gas phase by thermionic emission of the ions from a heated metal filament painted with the alkali ion salts.^{9,10} This apparatus was dismantled several years ago. Recently, the electrospray (ES) method with which ions present in a solution

can be transferred into the gas phase and subjected to mass spectrometric detection, was developed by Fenn and co-workers.¹¹ Electrospray affords the production not only of ions such as Na^+ and K^+ and other singly charged ions but also that of doubly and triply charged transition metal and alkaline earth ion–ligand complexes,¹² multiply protonated peptides and proteins,¹³ doubly charged anions¹⁴ like SO_4^{2-} and HPO_4^{2-} , and multiply deprotonated nucleic acids.¹⁵ The latter are also of paramount importance in solution chemistry and biochemistry but could not be obtained in the gas phase prior to the development of ES.

ES generates ions in ambient gas at ~ 1 atm, and the determination of ion concentrations with a mass spectrometer in gas at such high pressure is difficult. A successful design where the gas is transferred to a reaction chamber at 5–10 Torr pressure, where the ion–molecule equilibria establish, was described recently.¹⁶

The ion–equilibrium method is not well suited for determinations where the bond enthalpies are high, i.e. greater than ~ 40 kcal/mol, because of the very high temperatures required for the equilibrium to establish. However, many ion–ligand complexes can have such high bond enthalpies particularly when multiply charged ions are involved.¹¹ Therefore, it is very desirable to have a method with which the bond energies of strongly bonded ion–ligand complexes, produced by electrospray, can be determined.

Determination of the threshold of the product ion, M^+ , where the reactant ion, ML^+ , is accelerated to known kinetic energies, experiences a collision with a noble gas atom and undergoes dissociation, is a method with which bond enthalpies, e.g., ΔH°_1 values, can be determined. This collision-induced dissociation (CID) threshold method^{18,19} is applicable also when high bond energies are involved. The present work describes some of the first results with this method as applied to ions generated by ES. The determinations for M^+ (Na^+ , K^+) and L (acetamide, AA; *N*-methylacetamide, MAA; and *N,N*-dimethylacetamide, DMA) are described in subsequent sections.

Determinations for K^+ and $L =$ acetone and dimethyl sulfoxide were also made for the purpose of comparing the CID threshold data with available previous determinations based on ion equilibria. Determinations involving Na^+ and K^+ and $L =$ glycine, glycine amide, succinamide, and the dipeptide, glycyglycine, were also made. The last three ligands may lead to

[⊗] Abstract published in *Advance ACS Abstracts*, July 15, 1996.

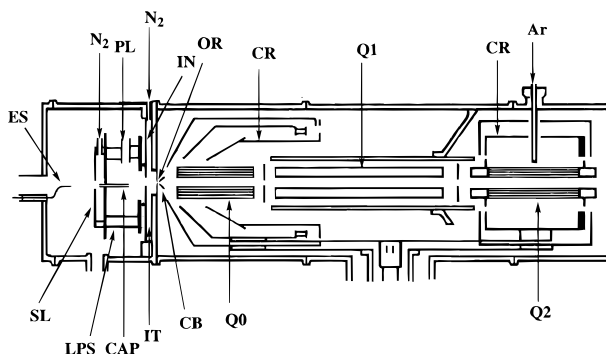


Figure 1. Front end apparatus. Electrospray generator, ES, consisting of electrospray capillary with stainless steel tip at high electric potential, generates charged droplets and ultimately gas phase ions. ES is partially surrounded by glass tube providing flow of dry air. Capillary, CAP, transfers gas and ions from 1 atm to a low pressure ion source LPS maintained at 10 Torr. Ions can be partially declustered by applying a high drift field between CAP and interface plate IN. Ions are allowed to thermalize in low drift field, 10 Torr pressure, ion thermalization chamber IT. Orifice OR, 100 μm diameter leads to vacuum. First electrode and skimmer, CB. RF only ion guide quadrupole Q_0 . First quadrupole Q_1 . Cryosurfaces CR for cryopumping.

bi- and tridentate complexes and provide an interesting extension of the CID threshold results.

Mass spectral analysis of electrospray produced ions from aqueous and methanol solutions containing low concentrations of peptides or proteins and Na^+ ions due to the presence of electrolytes $\text{Na}^+ + \text{X}^-$ in the solutions has shown¹¹ that the peptides and proteins form sodium ion adducts. Multiple sodium ion addition occurs with polypeptide and protein molecules. The number of sodium ions increases with the number of the peptide units in the molecule.¹¹ The sodium ions evidently form complexes with polar regions of the peptides, although the complexation may be largely occurring as a consequence of the ion transfer from solution to the gas phase. Therefore, data on the bonding forces between alkali ions and peptides or models of peptides, such as described in this work, are of interest also from the standpoint of electrospray mass spectrometry and the mechanism of electrospray mass spectrometry. One should not fail to notice that there are certain analogies between the transfer of sodium and potassium ions from solution to the transmembrane channels and the transfer from solution to the gas phase when the solution contains peptides or proteins.

Experimental and Curve-Fitting Procedure

(a) Apparatus and Conditions. As mentioned in the Introduction, with electrospray one obtains gas phase ions in ambient gas at 1 atm pressure. The transfer of these ions to the vacuum of the mass spectrometer used for the CID studies presents some special challenges because the accelerated ions entering the collision cell must have a known internal energy distribution, preferably a Maxwell–Boltzmann distribution at a known temperature. Furthermore, the translational kinetic energy of the ions must be well-defined and have a narrow distribution. The present measurements were performed with a modified triple quadrupole mass spectrometer.²⁰ A detailed account which describes how and to what extent the above challenges could be met is given elsewhere.²⁰ Here, we give only a brief description of the apparatus and conditions of the present measurements.

The mass spectrometer used was a SCIEX Trace Atmospheric Gas Analyzer 6000 E, triple quadrupole mass spectrometer.²¹ The front end was modified as shown in Figure 1. There are four sections:

(1) The electrospray generator, ES, produces charged droplets and ultimately gas phase ions from an electrolyte solution which flows through the ES capillary.

Solutions of electrolytes NaCl or KCl at 10^{-4} mol/L in methanol and the ligand L at 10^{-3} mol/L were used to generate the ions NaL^+ and KL^+ .

(2) The low-pressure ion source, LPS, is maintained at 10 Torr by means of a pump. Atmospheric pressure gas containing ES produced ions is admitted through the sampling capillary CAP. The clustered ions such as M^+L_n or $M^+L_n(\text{H}_2\text{O})_x$ entering the chamber can be partially declustered to a given desired species such as M^+L , by applying a high ion drift field between the tip of CAP and the bottom plate IN of the low-pressure source LPS.

(3) The ion thermalization chamber IT is at the same pressure as the low-pressure source. The ion drift field between IN and the orifice OR is low, $E/p < 6$ V/(cm Torr), so that thermalization of the ions can occur in this region.²⁰

(4) The triple quadrupole mass spectrometer is where ions entering the cryopumped vacuum region are subjected to mass analysis and CID. Precursor ions selected by Q_1 are accelerated to the RF only collision cell Q_2 where product ions are created by collisions with Ar gas. A given product ion is mass selected with Q_3 and detected with an ion counting system.

It was shown²⁰ that the precursor and product-ion kinetic energy profiles are independent of the potential difference CAP-IN used for the declustering of ions in the low-pressure ion source LPS. The profiles were also independent of the potential drop between IN and OR when $E/p < 6$ V/(cm Torr). This is consistent with the assumed ion thermalization in the IT chamber.

It was found²⁰ that the kinetic energy profiles of the precursor ions are somewhat broadened, i.e., develop a tail toward higher kinetic energies. The broadening increased with the magnitude of the radial dc field in the first quadrupole Q_1 . Collisions of the parent ions with neutral gas molecules of the gas jet present in Q_1 were assumed to be responsible for the broadening.²⁰ The broadening was reduced by working at low radial dc fields, i.e., low mass resolution in Q_1 . It was found, in the present work, that the broadening could be further reduced by selecting a specific offset potential for the Q_1 quadrupole, i.e. by controlling the axial kinetic energy of the precursor ions entering Q_1 . For an ion of mass to charge ratio $m/z = 110$, the selected kinetic energy was typically 12 eV. The selected energy decreased as m/z decreased. The exact cause for the observed behavior is under investigation.

It was also established²⁰ that collisions of the ions with gas molecules in the front end space between the electrodes OR, CB, and Q_0 lead to kinetic energy broadening. This broadening was eliminated by setting equal potentials to OR, CB, and Q_0 . While the mass analyzed parent ion intensity is reduced under these conditions, the signals obtained, $\sim 20\,000$ ions/s, are sufficient for the threshold measurements.

The collision gas argon was at a pressure of ~ 0.1 mTorr (collision cell length 8 cm). At such a pressure single collisions are dominant and the contribution of double collisions to the foot of the threshold curve are negligible. This was verified by making threshold measurements at decreasing pressures and observing that the E_0 value obtained increased by less than 0.02 eV for a decrease of the pressure from 0.2 to 0.1 mTorr.²⁰

(b) Determination of Threshold Energies E_0 . Determinations of the energy thresholds E_0 were obtained by fitting the product ion energy profiles with the CRUNCH program developed by Armentrout and co-workers.^{18,22} The fitting procedure is based on the equation

TABLE 1: Energies for the Reaction $M^+L = M^+ + L$ from CID Threshold Determinations^a

	$E_{0(0\text{ K})}^b$	$\Delta H^\circ_{298}^b$	$\Delta H^\circ_{298}^c$	$\Delta H^\circ_{298}^d$	ΔH°_{298} (lit.)
$M^+ = K^+$					
Me ₂ CO	24.2	24.4	24.4	24.4	26.0 ^e
Me ₂ SO	31.3	31.6	30.2	31.1	35 ± 3 ^e
HCONMe ₂	32.0	32.0	27.1	29.5	31.0 ^e
MeCONH ₂	29.7	29.6	29.6	29.7	(26.2) ^f
MeCONHMe	32.3	31.9	28.3	30.4	(24.8) ^f
MeCONMe ₂	32.9	32.2	25.5	29.0	31 ^e
H ₂ NCH ₂ COOH	29.2	30.1	29.4	30.0	
$M = Na^+$					
MeCONH ₂	34.3	34.7	34.7	34.7	(36.0) ^g
MeCONHMe	38.9	39.0	33.7	35.7	(38.4) ^g
MeCONMe ₂	46.9	46.7	35.2	37.5	
H ₂ NCH ₂ COOH	36.3	37.5	35.7	36.6	(38.5) ^h
H ₂ NCH ₂ CONH ₂	45.1	45.1	39.5	41.4	
(H ₂ NCOCH ₂) ₂	62.3	61.8	41.5	44.5	
H ₂ NCH ₂ CONH- CH ₂ COOH	64.6	64.7	40.1	42.9	

^a All energies in kcal/mol. ^b Without correction for kinetic shift, E_0 internal energy change, ΔH° enthalpy change for reaction eq 1. ^c With correction kinetic shift, two lowest frequencies, 30 cm⁻¹, for both K⁺ and Na⁺ complexes. ^d With correction for kinetic shift, two lowest frequencies, 10 cm⁻¹, for Na⁺ complexes and 5 cm⁻¹ for K⁺ complexes. This set is considered to be the best. ^e Experimental determinations based on ion-molecule equilibria (Sunner et al.).^{8 f} Theoretical calculations, HF/6-31G, combined with a semiempirical correction (Roux and Karplus).^{7 g} Theoretical calculations, HF/6-31G*, combined with a semiempirical correction (Roux and Karplus).^{7 h} Theoretical calculations, 6-31+G(2d)MP2 (Jensen).^{28 i} Succinamide.

$$\sigma = \sigma_0 \sum_i g_i (E + E_i + E_{\text{rot}} - E_0)^n / E \quad (2)$$

where σ is the cross section, which is proportional to the observed product ion intensity at single collision conditions. E is the kinetic energy in the center of mass frame. E_i is the internal vibrational energy of the precursor ion whose relative abundance at a given temperature is g_i , where $\sum_i g_i = 1$. E_0 is the threshold energy, corresponding to the energy required for the dissociation reaction, i.e., eq 1 in the present work, at 0 K.

The fitting procedure based on eq 2 treats n and E_0 as variable parameters which are determined through the best fit. The vibrational energies E_i are calculated from the frequencies of the normal vibrations of the precursor ion. The frequencies are generally obtained from quantum chemical calculations.

An important feature underlying eq 2 is the assumption that due to the relatively long residence time of the excited ions in Q₂, dissociation at the threshold involves the process where the internal energy of the products is close to 0 K, i.e., essentially all the internal energy of the precursor ion is used up in the dissociation at the observed threshold.

The observed precursor ion kinetic energy profiles were fitted to a Gaussian distribution and the zero center of mass kinetic energy was taken at the maximum of the Gaussian curve.

Results and Discussion

(a) Results: Evaluation of the Threshold Energies. Effect of Kinetic Shift. Threshold curves for the product ions Na⁺ and K⁺ from the dissociation of the sodium and potassium complexes M⁺L are shown in Figures 2–8. The values of the exponents n and the E_0 values obtained by fitting the data to the expression, eq 2, are given in the figures and Table 1. The vibrational frequencies for the M⁺L complexes required for the evaluation of the internal energies E_i , see eq 2, were obtained with ab initio calculations (3–21 G basis set) for Na⁺·CH₃CONH₂ and CH₃CONH₂ and the semiempirical MNDO for the

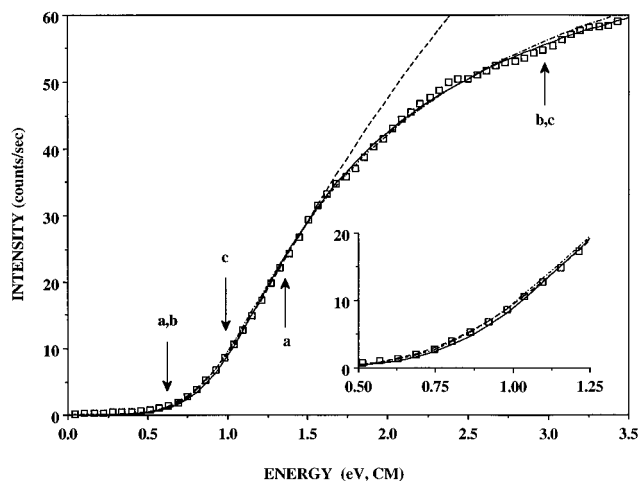


Figure 2. Appearance curve of K⁺ from CID of K⁺ acetone. Also shown are three calculated cross-section curves (a–c), obtained by fitting the cross-section model, eq 2, to different portions of the appearance curve. Curve a (—), fitted from 0.6 to 1.4 eV, corresponds to $n = 1.46$ and $E_0 = 0.99$ eV (22.8 kcal/mol). Curve b (— · —), fitted from 0.6 to 3.0 eV, corresponds to $n = 1.05$ and $E_0 = 1.09$ eV (25.1 kcal/mol). Curve c (—), fitted from 1.0 to 3.0 eV, corresponds to $n = 1.00$ and $E_0 = 1.11$ eV (25.5 kcal/mol). Expanded scale used for insert at lower right in figure provides a better view of the three curve fits at the threshold.

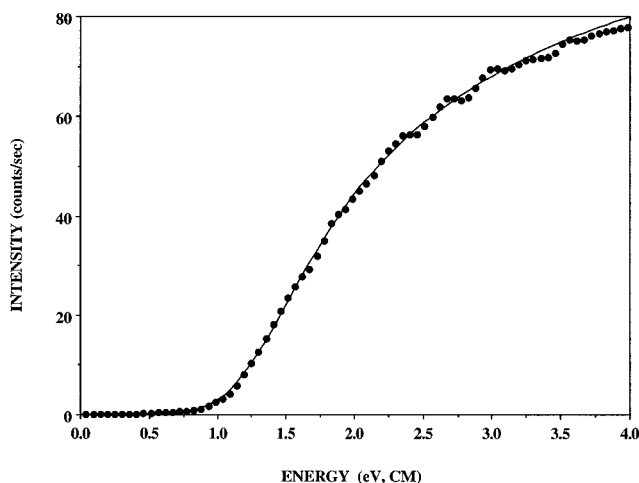


Figure 3. Appearance curve of K⁺ from CID of K⁺N-methylacetamide. The calculated curve (solid line), fitted from 1.1 to 2.5 eV, corresponds to $n = 1.02$ and $E_0 = 1.40$ eV (32.2 kcal/mol). Cross-section model, eq 2.

other reactants. The frequencies used are given in Table 2. A temperature of 298 K was assumed for the precursor ions.

Illustrations of alternate fitting results are given in Figure 2. The different values of n and E_0 for K⁺ (acetone) given in the figure result from different choices of the range of points, at the foot of the threshold and near the maximum of the cross section, which were included in the fit.

In general, we have excluded the experimental points of very low intensity at the very end of the foot because these probably originate from precursor ions of higher than thermal energies.²⁰ The very small difference observed between the E_0 values obtained for the fits b and c, E_0 (b) = 1.09 eV and E_0 (c) = 1.11 eV, which differ by points excluded at the foot, provide assurance that points of very low intensity at the foot can be excluded. The relatively close values for the fits a and b, E_0 (a) = 0.99 eV and E_0 (b) = 1.09 eV, demonstrate that inclusion of experimental points past the steeply rising portion of the curve does not affect the E_0 values very significantly. Thus, while there is a certain arbitrary element in the choice of the fit, the E_0 values agree within ~0.1 eV. The E_0 values quoted in Table

TABLE 2: Vibrational Frequencies^a

acetone ^b	K ⁺ acetone ^b	DMSO ^b	K ⁺ DMSO ^b	DMF ^c	K ⁺ DMF ^c			
	37		71		36			
	69		81		45			
	90		155		59			
86	150	148	187	82	80			
160	186	179	191	105	117			
406	425	220	263	149	182			
549	556	238	280	247	277			
553	561	304	315	335	341			
806	819	633	644	435	437			
981	991	700	700	649	654			
1019	1015	712	881	1024	1032			
1201	1203	1027	1040	1036	1036			
1257	1261	1061	1080	1160	1156			
1315	1337	1104	1121	1166	1160			
1553	1561	1155	1161	1169	1175			
1562	1573	1493	1499	1190	1189			
1627	1617	1520	1527	1404	1403			
1630	1622	1610	1604	1426	1426			
1638	1625	1623	1618	1431	1427			
1662	1655	1628	1618	1432	1428			
1940	1891	1643	1634	1433	1431			
3199	3204	3239	3243	1520	1511			
3206	3212	3240	3243	1527	1524			
3249	3258	3342	3350	1540	1537			
3258	3267	3342	3351	1567	1588			
3306	3307	3345	3353	2083	2043			
3307	3308	3347	3355	3215	3230			
				3217	3231			
				3236	3249			
				3247	3254			
				3267	3271			
				3308	3318			
				3325	3327			
AA ^b	K ⁺ AA ^c	Na ⁺ AA ^b	MAA ^b	K ⁺ MAA ^c	Na ⁺ MAA ^c	DMA ^d	K ⁺ DMA ^d	Na ⁺ DMA ^d
	44	92		29	55		25	40
	57	103		43	55		35	45
	67	124		57	101		47	80
147	142	328	108	103	111	108	203	111
451	360	489	137	131	133	108	103	111
530	417	591	194	173	174	137	131	133
590	448	609	308	302	304	194	173	174
596	583	710	457	423	457	194	173	174
735	616	849	619	156	159	308	302	304
874	1032	902	672	617	621	457	423	457
1090	1077	1128	682	651	652	619	156	159
1193	1099	1207	930	999	1000	672	617	321
1247	1220	1258	1051	1085	1085	682	651	352
1442	1425	1530	1190	1098	1098	930	999	1000
1556	1436	1571	1192	1172	1170	1051	1085	1085
1637	1483	1628	1262	1234	1233	1051	1085	1085
1658	1542	1650	1289	1311	1308	1190	1098	1098
1814	1804	1806	1380	1421	1421	1192	1172	1170
1917	2056	1846	1554	1424	1422	1262	1234	1233
3208	3268	3215	1596	1425	1423	1289	1311	1308
3263	3276	3276	1630	1438	1436	1289	1311	1308
3337	3346	3327	1658	1472	1476	1380	1421	1421
3784	3608	3748	1663	1492	1482	1554	1425	1422
3910	3630	3866	1686	1530	1530	1554	1424	1422
			1708	1702	1707	1596	1425	1423
			1895	2043	2040	1630	1438	1436
			3198	3229	3233	1658	1472	1436
			3205	3257	3259	1663	1492	1476
			3248	3269	3269	1663	1492	1476
			3262	3278	3279	1686	1530	1482
			3322	3328	3328	1686	1530	1530
			3344	3349	3349	1708	1702	1707
			3807	3575	3568	1895	2053	2040
						3198	3229	3233
						3205	3229	3259
						3248	3257	3269
						3198	3257	3233
						3205	3269	3259
						3248	3269	3269
						3262	3278	3279
						3322	3328	3328
						3807	3575	3568

TABLE 2 (Continued)

glycine ^c	K ⁺ glycine ^c	Na ⁺ glycine ^c	glycinamide ^c	Na ⁺ glycinamide ^c	succinamide ^c	Na ⁺ succinamide ^c	Gly ₂	Na ⁺ Gly ₂ ^e
	23	39		50		31		39
	53	59		73		49		42
	57	84		94		69		63
65	65	103	54	103	18	77	35	72
162	232	218	227	193	36	100	42	92
295	300	307	294	291	167	103	56	96
427	426	459	372	410	235	220	99	98
476	498	533	431	441	267	275	167	157
590	589	592	567	498	321	380	226	221
741	739	674	689	577	414	390	287	248
991	987	988	783	742	433	429	324	365
1000	1003	1002	987	977	490	451	454	399
1118	1148	1169	989	991	501	501	485	486
1214	1213	1222	1128	1123	529	518	510	528
1302	1310	1322	1214	1190	540	582	540	549
1363	1636	1367	1262	1228	589	589	588	604
1417	1390	1387	1298	1316	596	694	612	624
1462	1456	1429	1359	1364	740	755	638	660
1474	1471	1477	1457	1453	922	901	703	766
1596	1609	1619	1466	1471	935	939	917	872
1810	1810	1805	1513	1553	1048	1058	953	943
2109	2084	2074	1812	1808	1065	1067	1006	962
3192	3195	3206	1813	1811	1143	1168	1039	1030
3279	3255	3272	2098	2045	1181	1196	1070	1055
3536	3538	3534	3206	3200	1194	1216	1161	1164
3587	3581	3585	3272	3266	1208	1231	1195	1199
3953	3974	3930	3551	3547	1246	1264	1256	1272
			3579	3593	1366	1404	1315	1313
			3594	3613	1379	1415	1339	1336
			3606	3627	1398	1458	1345	1349
					1404	1466	1381	1356
					1561	1538	1408	1418
					1564	1546	1431	1434
					1704	1806	1455	1442
					1705	1809	1474	1472
					1985	2054	1547	1575
					2000	2071	1644	1657
					3015	3222	1724	1722
					3019	3236	2001	1961
					3081	3293	2081	2062
					3093	3303	2952	2944
					3487	3592	2958	2980
					3524	3607	3024	3013
					3542	3635	3028	3038
					3546	3636	3416	3384
							3437	3441
							3475	3446
							3481	3486

^a The vibrational frequencies (in cm⁻¹) of the ligand and ion–ligand complexes were obtained by evaluating the Hessian of the corresponding optimized geometries using the GAMESS program. Only frequencies below 1000 cm⁻¹ are significant in the fitting procedure, eq 2, and in the calculation of the internal energies needed in eq 3. Furthermore, the fitting procedure and internal energy calculations are not sensitive to the values of the frequencies and errors of 20% are expected to have only a small effect on the energy determinations. ^b The vibrational frequencies were obtained from HF calculations done using a 3-21G basis set. ^c The vibrational frequencies were obtained from semiempirical calculations (MNDO). ^d The frequencies for CH₃CON(CH₃)₂ (DMA), K⁺CH₃ON(CH₃)₂ (K⁺DMA), and Na⁺CH₃CON(CH₃)₂ (Na⁺DMA) were estimated by comparing the calculated frequencies for CH₃CONH₂ (AA) and CH₃CONHCH₃ (MAA) and the corresponding metal ion complexes. ^e The frequencies for H₂NCH₂CONHCH₂COOH (Gly₂) and Na⁺Gly₂ were obtained from semiempirical calculations (AMI).

I correspond to the averages between two or three of the fits, considered as best. We assign an error of ±0.1 eV to these results.

We have included the thermal rotational energy of the precursor ion, $E_{\text{rot}} = 3/2RT$, see eq 2, in our curve-fitting procedure. Armentrout et al.²⁴ who fit the threshold curves right to the very bottom of the threshold, do include this term. Squires et al.,¹⁹ who omit points from the bottom i.e., the foot of the curve, which are presumed to be due to above thermal ions, do not include the rotational energy, making the assumption that the rotational energy will affect only the bottom of the curve, i.e., the portion that is omitted from the fit. Since in our experiments we also do not fit the foot of the curve, following Squires et al., we should have omitted the rotational energy. However, the transition states involved in the present work, vide infra, are expected to have two very large moments of inertia, and since the angular momentum quantum number

is conserved, a decrease of rotational energy for these rotations is expected and this energy will be converted into internal energy, on formation of the transition state. Therefore, these two rotational energy terms $^{2/2}RT$ should be included in the fit. For simplicity, we have included $^{3/2}RT$.

The E_0 values, which correspond to the dissociation energy at 0 K, were converted to enthalpy changes at $T = 298$ K, with use of eq 3 (Armentrout²²).

$$\Delta H^\circ = E_0 - E_{\text{vib}}(\text{ML}^+) + E_{\text{vib}}(\text{L}) + ^{5/2}RT \quad (3)$$

Equation 3 is based on a thermodynamic cycle for the enthalpy change, ΔH° , of reaction 1 between 0 and T K. The required vibrational thermal energies $E_{\text{vib}}(\text{ML}^+)$ and $E_{\text{vib}}(\text{L})$ were evaluated from the corresponding vibrational frequencies which are given in Table 2. Due to cancellation of heat capacity terms

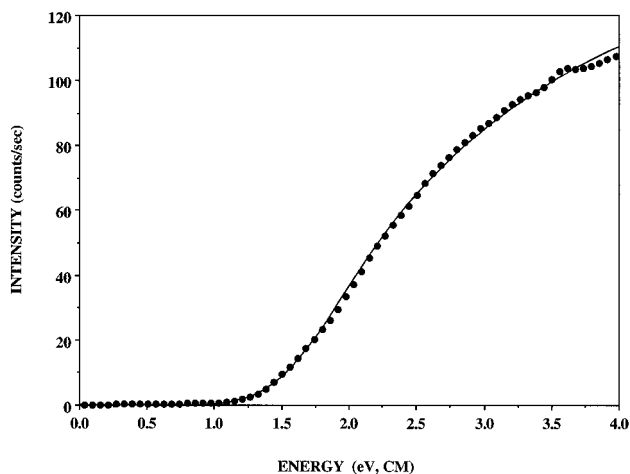


Figure 4. Appearance curve of Na^+ from CID of Na^+N -methylacetamide. The calculated curve (solid line), fitted from 1.4 to 4.0 eV, corresponds to $n = 1.25$ and $E_0 = 1.69$ eV (38.9 kcal/mol). Cross-section model, eq 2.

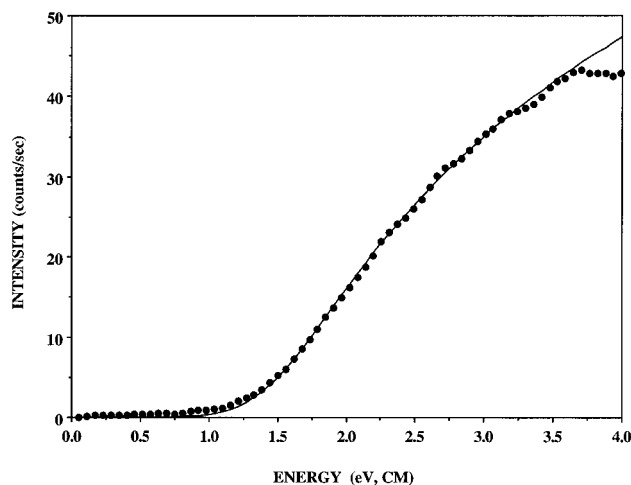


Figure 7. Appearance curve of Na^+ from CID of Na^+ glycine. The calculated curve (solid line), fitted from 1.6 to 3.4 eV, corresponds to $n = 1.20$ and $E_0 = 1.58$ eV (36.3 kcal/mol). Cross-section model, eq 2.

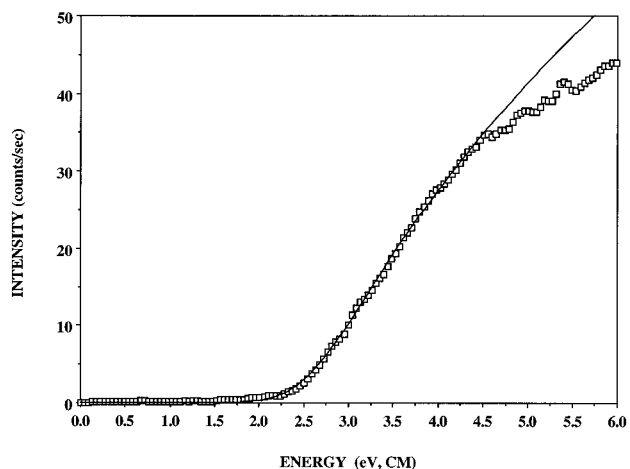


Figure 5. Appearance curve of Na^+ from CID of Na^+ succinamide. The calculated curve (solid line), fitted from 2.8 to 4.5 eV, corresponds to $n = 1.25$ and $E_0 = 2.70$ eV (62.3 kcal/mol). Cross-section model, eq 2.

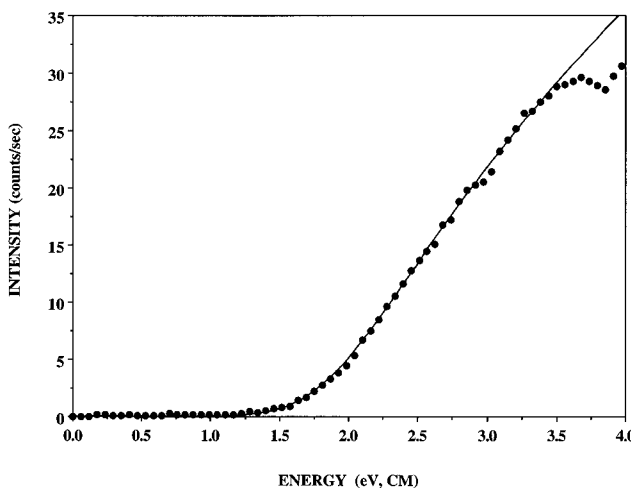


Figure 8. Appearance curve of Na^+ from CID of Na^+ glycinamide. The calculated curve (solid line), fitted from 2.0 to 3.5 eV, corresponds to $n = 1.31$ and $E_0 = 1.96$ eV (45.1 kcal/mol). Cross-section model, eq 2.

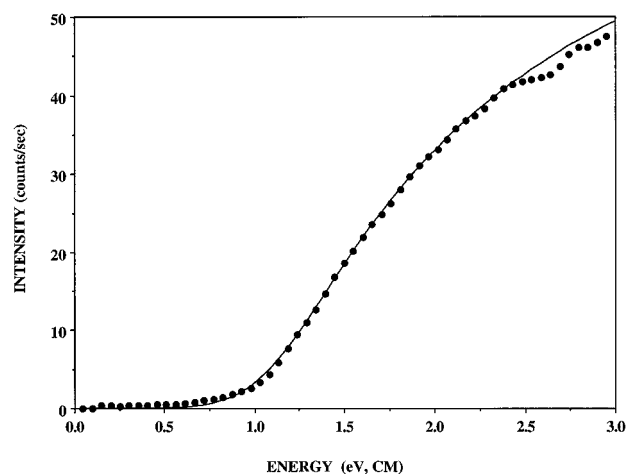


Figure 6. Appearance curve of K^+ from CID of K^+ glycine. The calculated curve (solid line), fitted from 1.2 to 2.0 eV, corresponds to $n = 1.07$ and $E_0 = 1.27$ eV (29.2 kcal/mol). Cross-section model, eq 2.

in the cycle, the values of E_0 at 0 K and ΔH° at 298 K turn out to be very similar.

The fits of the experimental profiles with eq 2 are based on the assumption that the energized reactant ions, whose total energy is equal or larger than E_0 , will decompose within the

residence time t of the ion before entering the mass analyzer Q_3 . For the present apparatus, t is estimated to be between 30 and 40 μs and complete dissociation within that time, for ions with energies just above E_0 can be expected only for relatively small polyatomic ions. Ions with many internal degrees of freedom will attain the required dissociation rate only at internal energies which are somewhat higher than E_0 . This "kinetic shift",²³ if not taken into account, will lead to E_0 values that are too high.

Armentrout et al.²⁴ have developed a method with which the kinetic shift can be taken into account in the curve-fitting procedure. This fitting procedure includes only to the fraction of the precursor ions which decompose during the residence time t . This fraction is given by, $1 - \exp(-kt)$, where k is the rate constant for the decomposition. k can be evaluated with the RRKM formalism.²⁵ k is a function of the internal energy of the ion and the threshold energy E_0 , i.e., $k(E + E_i - \Delta E - E_0)$, where E is the kinetic energy in the centre of mass frame, E_i is the internal energy of the ion prior to the collision, and ΔE is the center of mass kinetic energy which was not converted into internal energy of the ion. The dependence of ΔE on the center of mass energy, E , was obtained²⁴ on the basis of an assumed relationship, since an accurate theoretical expression for that dependence is not available.

For the evaluation of k with RRKM one needs to know the vibrational frequencies of the transition states occurring in reactions eq 1. These were estimated as follows. Examination of the frequencies of the M^+L species in Table 2 shows that these contain three lowest frequencies which are associated with motions of M^+ relative to L , while the rest of the frequencies are all quite close to those of L . Since the transition state for the dissociation is a "late" transition state which resembles the separated M^+ and L , its frequencies can be obtained by dropping one of the three low frequencies of M^+L and reducing the remaining two to low values. Energy changes, based on fits of the experimental threshold curves obtained with this procedure, are given in Table 1.

The energy values obtained with the correction for the kinetic shift are dependent on the choice of the value of the two lowest frequencies of the transition state. Two sets of kinetic shift corrected ΔH° values are given in Table 1. The first set uses 30 cm^{-1} for all K^+ and Na^+ complexes. This frequency was based on the choice of 25 cm^{-1} made by Wenthold and Squires in a study of the CID of chlorophenyl radical anions²⁶ leading to Cl^- as product ion where a late transition state is also expected to occur. The authors²⁶ made the choice of 25 cm^{-1} on the basis of literature data for experimentally measured ΔS^\ddagger values of similar reactions.

There are significant differences between the chloride dissociation and the dissociation of the alkali ion–ligand complexes. The ion–dipole and induced dipole interactions which dominate the bonding in the alkali complexes involve weaker but longer range forces. Furthermore, the bonding modes involving the alkali ion and the ligand have lower frequencies due to the less directional character of the electrostatic, relative to the covalent bond. At the large distances between the ligand and the alkali ion expected for the transition state, the frequencies associated with the bonding should be considerably lower than is the case for the chlorophenyl anion transition state.

To obtain frequencies for a looser transition state, the following procedure was used. *ab initio* calculations at the 3–21 G level of the energies and frequencies of the complex, $Na^+\cdot CH_3CONH_2$ were performed for different ion–oxygen atom distances extending from the equilibrium distance (2 \AA) to a maximum distance of 14 \AA . For this distance, the bond energy of the complex had reduced to $\sim 2\%$ of the equilibrium distance energy. At this distance, the average of the two lowest frequencies, which did not correspond to the reaction coordinate, was $\sim 10\text{ cm}^{-1}$. Assuming that the contribution of the rotational barrier to the transition state energy is very small, such that the transition state occurs very near to the complex dissociation, the value of 10 cm^{-1} can be adopted for the two lowest transition state frequencies. For the K^+ complex, the frequencies should be somewhat lower and a value of 5 cm^{-1} was chosen. ΔH° values obtained with these frequencies for all the Na^+ complexes and K^+ complexes are given in Table 1; see second last column, ΔH° .

The entropy change associated with the formation of the transition state at 1000 K, ΔS^\ddagger_{1000} , is often quoted²⁶ and used as a measure of the "looseness" of the transition state, where a loose transition state is assumed to have a value, $\Delta S^\ddagger_{1000} > 0$. The vibrational frequencies used for the transition state of $Na^+\cdot CH_3CONH_2$, lead to a $\Delta S^\ddagger_{\text{vib}} \approx 3.7\text{ cal}/(\text{deg}\cdot\text{mol})$. The transition state has two moments of inertia which are much larger than those for the precursor ion and this rotational change leads to $\Delta S^\ddagger_{\text{rot}} \approx 5\text{ cal}/(\text{deg}\cdot\text{mol})$, for a total of $\Delta S^\ddagger_{1000} = 8.7\text{ cal}/(\text{deg}\cdot\text{mol})$. This value corresponds to a very loose transition state and appears appropriate for the electrostatically long range bonding prevailing in the present ion–ligand complexes.

Comparison of the ΔH° data without and with kinetic shift correction, Table 1, provides an illustration for the magnitudes of the corrections. The corrections for small ligands, Me_2CO , Me_2SO , $MeCONH_2$ are small, i.e., less than 1 kcal/mol , and the exact value of the frequencies used is not important. Larger corrections are required for the bigger and the more strongly bonded ligands. Succinamide (H_2NCOCH_2)₂ is an extreme case where the strong bonding and the large size of the ligand require a correction which is $15\text{--}20\text{ kcal/mol}$. Due to the uncertainty of the choice for the transition state frequencies, the ΔH data for this compound might be in error by as much as $\pm 5\text{ kcal/mol}$.

The choice of the two lowest frequencies for the Na^+ complexes (10 cm^{-1}) and K^+ complexes (5 cm^{-1}), although justified to a certain extent in the discussion above, is also a semiempirical choice. As will be seen in the next section, these values lead to the closest agreement with available ΔH° data in the literature.

A somewhat different procedure was used in a very recent CID threshold study of $Li^+(\text{CH}_3\text{OCH}_3)_x$ complexes, by Armentrout and co-workers.²⁷ These authors also used the frequencies of the complex as the starting point for the transition state frequencies. For $x = 1$, they dropped the frequency which corresponded to the reaction coordinate and divided the two other lowest frequencies by 2 and by 10 obtaining thus two sets of frequencies. The two threshold values obtained with these two choices were considered as the limits of the true value.

The quadrupole collision cell used in the present work has some drawbacks relative to the octapole cell used by Armentrout and co-workers.¹⁸ These have been discussed.¹⁸ The major advantage of the octapole is the type of energy well that it produces. The ac potential well in the octapole increases very slowly, inverse sixth power, with radial distance R , from the octapole axis, while in the quadrupole, this field increases much faster, with the inverse square power of R . The flat bottom of the octapole well leads to a lesser pickup of kinetic energy in the radial direction by ions which are off center from the multipole axis. Part of the tailing toward low energies observed in the threshold curves Figures 2–8 is undoubtedly due to pickup of such kinetic energy in the quadrupole cell Q₂. However, the tailing is small and can be avoided by omitting points at very low energies; see Figures 2 and 3 and discussion. Evidence that the tailing due to excess internal energy in the precursor ions is small is provided by a comparison of the theoretical fit based on eq 2 and the experimental points; see Figures 2–7. The experimental points at the very onset coincide quite closely with the threshold fit. While the accuracy achieved with the quadrupole trap is lower than that obtained with the apparatus of Armentrout,¹⁸ the main uncertainty in the data obtained for the measurements which involve larger molecules is not the energy spread but the modeling of the kinetic shift.

Squires and his co-workers¹⁹ who have used a triple quadrupole for threshold measurements for many years have shown that such an apparatus can provide many measurements of great interest, with sufficient accuracy. The present apparatus allows threshold measurements involving a large variety of ions that at present can be obtained only by electrospray. We believe this capability justifies its use even at the cost of some reduced accuracy of the measurements.

(b) Comparison of Threshold-Based Energies with Literature Data. Types of Bonding Present in the Complexes. The ΔH°_{298} data obtained from the CID thresholds, discussed in the preceding section, can be compared with previous determinations in the literature.^{7,8,28} Previous determinations are available from ion equilibria studies⁸ for complexes of potassium with acetone, dimethyl sulfoxide, dimethylformamide,

and dimethylacetamide (Table 1). There is relatively good agreement between the equilibrium derived ΔH° values and the present CID results, particularly so with the set shown in the second last column, ΔH° , which we consider as the best values and which were obtained with the low-frequency choice for the transition states. These CID values are found to be ~ 1.5 kcal/mol lower than the equilibrium data. Only for dimethyl sulfoxide is there a larger difference of ~ 4 kcal/mol. However, the error limits given for the dimethyl sulfoxide equilibrium determination⁸ are quite high, ± 3 kcal/mol. Examination of the original data⁸ indicates that the slope of the van't Hoff plot was based on experimental points covering a narrow temperature range. In such cases, the ΔH°_1 values obtained are less certain than the ΔG° values at the experimental temperature. The experimental points⁸ are also compatible with a lower ΔH°_1 and a lower ΔS°_1 value. A lower ΔH°_1 value is also suggested by a correlation with lithium ion affinities determined by Taft and co-workers.^{29,30} A plot of the Li^+ affinities²⁹ vs ΔH°_1 values involving K^+ complexes determined by ion equilibria⁸⁻¹⁰ leads to a fairly good correlation. This correlation indicates for $L = Me_2SO$ a value of $\Delta H^\circ_1 \approx 31$ kcal/mol, while the value $\Delta H^\circ_1 = 35$ kcal/mol lies outside the curve. We conclude that the CID threshold result of 31.1 kcal/mol is to be preferred over the equilibrium value.⁸

Energy values from theoretical calculations, HF/6-31G, obtained by Roux and Karplus⁷ are available for K^+ and $L =$ acetamide (26.2 kcal/mol) and *N*-methylacetamide (24.8 kcal/mol). Both of these values are lower than the threshold results (29.7 and 30.4 kcal/mol). However, the authors⁷ were primarily interested in developing pair potential functions for molecular dynamics simulations and therefore did not refine their ab initio calculations as much as they could have. The values⁷ quoted in Table 1 are not the actual ab initio results which were considerably higher, but results obtained after a semiempirical correction based on the experimental and theoretical dipole moment.⁷ Therefore, we believe that the CID threshold results are to be preferred.

Roux and Karplus⁷ have obtained energy values (HF/6-31G*) also for the sodium ion complexes with acetamide (36.0 kcal/mol) and *N*-methylacetamide (38.4 kcal/mol). Also in this case, the semiempirical correction was applied to obtain the quoted results. These results are somewhat higher than the threshold values of 34.7 and 35.7 kcal/mol. Again, we believe that the threshold results should be preferred.

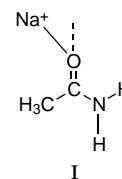
A theoretical result obtained by Jensen²⁸ is available for the complex of the sodium ion with glycine (H_2NCH_2COOH). The calculations performed at the MP2/6-31G* and MP2/6-31+G-(2d) level predict a complexation energy of 38.5 kcal/mol. A zero point energy correction was not included, but the correction should be small. Also, the conversion from ΔE at 0 K to ΔH° at 298 is expected to be small (~ 1.2 kcal/mol) (Table 1). This theoretical result, which is $\sim 2-3$ kcal/mol higher than the threshold result (36.6 kcal/mol), is within the expected combined error limits of the two determinations. Bouchonnet and Hopilliard³¹ have also performed calculations for the Na^+ -glycine complex. These authors carried their calculations only to the MP2/6-31G* level at which they obtained an energy of 45.2 kcal/mol. A very similar result (46.0 kcal/mol) was obtained by Jensen²⁸ with the same basis set. However, when the calculation was carried to the higher, MP2/6-31G+(2d) level, Jensen obtained the value, 38.5 kcal/mol, which is quoted in Table 1 and used in the present discussion.

The structures of the sodium and potassium ion complexes and their relationship to the observed bond energies are of interest and will be discussed in the following text. All ligands in Table 1 except dimethyl sulfoxide, which will not be

discussed, can be considered as substituted carbonyl compounds. Because of the expected dominance of electrostatic interactions and the large bond dipole and polarizability of the carbonyl group, the major contribution to the bonding in the complex should be due to this group. The other polar groups i.e. $-NH_2$, $NHCH_3$, $N(CH_3)_2$, and OH , also make contributions to the bonding as indicated by the observed changes of ΔH°_1 values in Table 1.

Acetone may be considered as the simplest of the ligands involved. Unfortunately, recent theoretical results for the structure and energies of the acetone sodium and potassium ion complexes do not seem to be available. Early work³² for the Na^+ complex predicts that the ion lies on the same axis as the C—O bond, as expected on the basis of electrostatics. The same structure can be expected for the potassium complex.

The bond with acetamide as the ligand is stronger. An increase from 24.4 kcal/mol (acetone) to 29.7 kcal/mol (acetamide) is observed for the potassium ion complexes (Table 1). The theoretical calculations of Roux and Karplus⁷ predict a structure in which the Na^+ ion is close to coaxial with the C—O bond. There is a tilt of a few degrees away from the C—O axis, in the plane of the N—C—O atoms as shown in structure I. This tilt approximately aligns the ion with the axis of the



molecular dipole of acetamide, which is due to the combined effect of the C—O and the C—N partial charges, the latter being due to the partial electron pair shift from the lone pair of the nitrogen to form a partial C—N π bond.

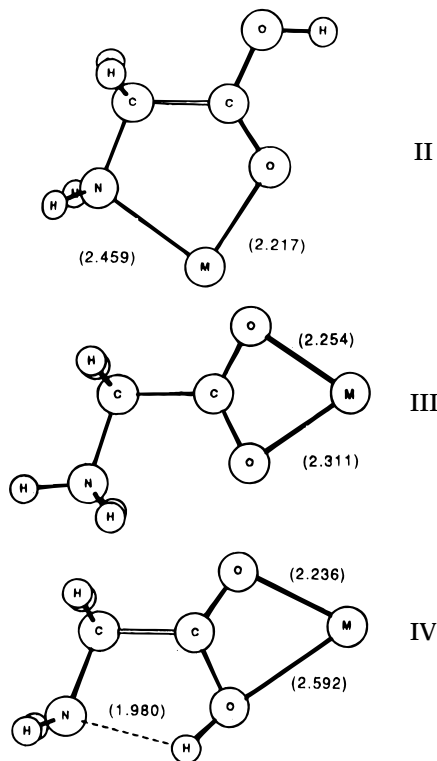
Substitution of H with methyl on the nitrogen in acetamide may be expected to strengthen somewhat the interaction with the sodium and potassium ion due to electron donation by the methyl group and to the increased polarizability of the ligand. Lithium ion affinities determined by Taft et al.^{29,30} exhibit such increases. Thus, the Li affinity increases by ~ 3.4 kcal/mol from acetamide to *N,N*-dimethylacetamide.²⁹ For Na^+ this value may be expected to become reduced by a factor of $\sim 2/3$ on the basis of comparisons between energies of Li^+ and Na^+ complexes.³³ This leads to an expected increase of 2.3 kcal/mol between Na^+ acetamide and Na^+ dimethylacetamide which is close to the observed difference of 2.8 kcal/mol between the corresponding ΔH°_{298} values in column 5 of Table 1. It is important to note that in the absence of a kinetic shift correction (see ΔH°_{298} in column 3) an increase of 12 kcal/mol would have been predicted which is clearly an erroneous result.

Methyl substitution in the potassium acetamide complexes should have a smaller effect roughly $1/2$ to $2/3$ of the effect expected for sodium because of the increasing remoteness of the methyl groups from the positive charge. On this basis, one can expect an increase by ~ 1.5 kcal/mol for two methyl substitutions. The observed ΔH°_{298} (column 5) values are 0.7 kcal/mol increase for the first methyl and a decrease of 1.4 kcal/mol for the second methyl. This is probably an erroneous trend but the expected changes are small, i.e., within the experimental error of ± 3 kcal/mol of the threshold determinations.

The threshold energies of the Na^+ or K^+ complexes with acetic acid were not determined. They are expected to be lower than those for acetamide because the more electronegative oxygen atom leads to significantly lower π and σ electron donation from $-OH$ relative to $-NH_2$. The relatively high ΔH°_1 values observed for the complexes of K^+ and Na^+ with

the α amino acetic acid (glycine) indicate that the α amino group makes an important contribution to the bonding of the complex and this suggests dicoordination involving the carbonyl and the amino group as shown in structure II.

The theoretical calculations for the sodium glycine complex by Jensen²⁸ at the MP2/6-31G* level predict structure II to be the most stable one. The distances, shown in Å, indicate a stronger bond to the carbonyl oxygen. Two other structures, III and IV, have only slightly lower stabilities. The glycine

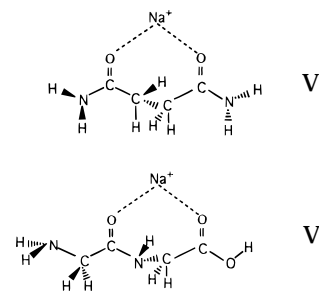


zwitterion structure III is only 2.2 kcal/mol higher in energy while the related structure IV in which a proton transfer has not occurred but a hydrogen bond interaction is present is higher by 4.7 kcal/mol.²⁸ Very similar results were obtained also by Bouchonnet and Hoppilliard.³¹ The variety of interactions leading to similar bond energies is interesting. Thus, the lowest energy structures II and III provide information on the interactions of a sodium ion with the N-terminal (structure II) and C-terminal (structure III) of neutral peptides.

The bond energy of the glycinamide complex with sodium was also determined (Table 1). The enthalpy change obtained is 41.4 kcal/mol, which is close to 6 kcal/mol higher than the 36.6 kcal/mol value observed for the sodium glycine complex (Table 1). As pointed out above, a higher value is expected because the amide NH_2 group is a better π and σ electron donor than the $-\text{OH}$ group of glycine.

Threshold-based enthalpy changes for the sodium ion complexes with the dipeptide glycyglycine and the diamide of succinic acid (succinamide) were also obtained (Table 1). Theoretical calculations for these complexes are not available in the literature. Probable structures for the two complexes are shown below. Structure V for the succinamide is based on an optimized MNDO geometry determination, and structure VI was obtained using the AM1 method.

The enthalpy change obtained for dissociation of the succinamide complex is $\Delta H^\circ_1 = 44.5$ kcal/mol (Table 1). One can examine whether this value is reasonable. Geometric constraints in structure V hinder the optimum orientation of the two carbonyl groups relative to the Na^+ ion. Such an optimum orientation can be achieved by two separate acetamide mol-



ecules, and the bond energy of such a complex would set the upper limit for the energy of the sodium succinamide complex. Data for the complexation of a second ligand molecule are often available from ion equilibria measurements.^{8-10,34} Unfortunately, such results are not available for the sodium ion and acetamide. However, data are available for sodium and acetone.³⁴ These show that the enthalpy required to fully dissociate the two acetone complex equals 1.75 times the enthalpy for the dissociation of the one molecule complex. Applying this factor to sodium and acetamide and using $\Delta H^\circ_{298} = 34.7$ kcal/mol, (column 5 of Table 1) one obtains 60.7 kcal/mol as an upper limit for the dissociation of the sodium succinamide complex. The experimental value, $\Delta H^\circ_{298} = 44.5$ kcal/mol (column 5 of Table 1) equals approximately 75% of the upper limit. The orientation of the two C–O dipoles in structure V is far from optimal and a bond energy that is $\sim 75\%$ of the optimal energy appears quite reasonable.

The structure VI shown for the sodium–glycyglycine complex indicates strong interactions only with the two carbonyl groups. Examination of space models of glycyglycine indicates that an alignment of the three groups: the two carbonyl groups and the terminal amino group, leading to interactions with the sodium as a tridentate complex, cannot be achieved.

The bond energy of complex VI is expected to be fairly close to that of the succinamide complex V, i.e., 44.5 kcal/mol. A somewhat smaller bond energy is expected for structure VI on the basis that succinamide has two NH_2 groups acting as π and σ electron donors while in glycyglycine there is only one amino group and a weaker donating hydroxy group. The value obtained, $\Delta H^\circ_1 = 42.9$ kcal/mol (column 5 of Table 1), is smaller, in agreement with the expected substituent effects.

On the basis of the above considerations, one may conclude that the interactions of a sodium ion with two adjacent carbonyl groups in a polypeptide will be somewhat stronger than those observed for the glycyglycine complex and very close to those for the succinamide complex because in the polypeptide and the succinamide complex stabilization is provided by two amide nitrogens.

Very recent and as yet unpublished work by Beauchamp and co-workers³⁶ has provided evidence that the most stable structures of the sodium ion complexes with the tri and higher polyglycines are zwitterion structures. These are similar to structure III for glycine but include an additional interaction where the terminal ammonium group is close to and thus stabilizes the negatively charged carboxy group. No results for glycyglycine are available yet.³⁶ If the zwitterion is the most stable structure also for glycyglycine, then the arguments given above concerning the agreement between the observed ΔH and expected bonding for structure VI will be invalidated, but only partially. Theoretical calculations³⁶ for the two structures indicate that the zwitterion is lower in energy but not by much; see also structures II and III due to Jensen²⁸ which were very close in energy as discussed above. This “coincidence” of energies would partially validate the discussion of structure VI. The closeness of the ΔH values for the sodium complexes with

succinamide where a zwitterion structure is not expected and glycylglycine also supports this view.

Assuming that the glycylglycine complex has the zwitterion structure, one might be concerned that structure VI will not provide the correct frequencies for the threshold fitting procedure. However, the frequencies of the zwitterion structure and structure VI will not be all that different and since the fitting procedure is not very sensitive to the frequencies, the error will be small. Concerning the transition state, the choice of frequencies will be the same for both cases.

One may ask whether the gas phase experiments can be extended to complexes which more closely model the interactions of the sodium and potassium ions in the gramicidin channel. Achieving a close correspondence seems impossible at the present time. However, the gas phase experimental data may provide some limiting complexation energy values. According to 2D NMR evidence³⁵ and theoretical work,²⁻⁴ the ion-channel interactions are principally due to interactions with four carbonyl oxygens of the peptide backbone and two water molecules which accompany the ion. A crude model for the optimum complexation energy may be provided by the complexation energy of the sodium ion with two suitable dicarbonyl molecules, such as glycylglycine amide (GGAm) and two water molecules, leading to $Na^+(GGAm)_2(H_2O)_2$. Experimental work presently underway in our laboratory has shown that such a complex can be produced in the gas phase. The dihydration of the complex $Na^+(GGAm)_2$ can be determined by ion equilibria measurements,¹⁶ while the complexation energies of the $Na^+(GGAm)_2$ would be amenable to CID threshold measurements and also ion molecule equilibria, for the addition of the second, less strongly bonded GGAm molecule. Determination of the free energy changes rather than only the enthalpy changes will be desirable because the transfer of the sodium ion from an aqueous medium to the transmembrane channel depends on the free energy change.

Acknowledgment. The present work was supported by grants from the Canadian National Sciences and Engineering Research Council NSERC. The authors are indebted to Professor P. Armentrout for making the CRUNCH program available to them and for informative discussions with Professor P. Armentrout and Professor R. R. Squires. The authors are also indebted to Professor B. Roux, who provided the impetus for this study.

References and Notes

- Andersen, O. S. *Annu. Rev. Physiol.* **1984**, *46*, 531.
- Pullman, A. *Q. Rev. Biophys.* **1987**, *20*, 173.
- Jordan, P. C. *J. Phys. Chem.* **1987**, *91*, 6582.
- (a) Roux, B.; Karplus, M. *Biophys. J.* **1991**, *59*, 961. (b) Roux, B.; Karplus, M. *J. Phys. Chem.* **1991**, *95*, 4856. (c) Roux, B.; Karplus, M. *J. Am. Chem. Soc.* **1993**, *115*, 3250.
- Kistenmacher, H.; Popkie, H.; Clementi, E. *J. Chem. Phys.* **1973**, *58*, 1689. Chandrasekhar, J.; Spellmeyer, D. C.; Jorgensen, W. L. *J. Am. Chem. Soc.* **1984**, *106*, 903.
- Kebarle, P. *Annu. Rev. Phys. Chem.* **1977**, *28*, 445.
- (a) Roux, B.; Karplus, M. *J. Phys. Chem.* **1991**, *95*, 4856. (b) Roux, B.; Karplus, M. *J. Am. Chem. Soc.* **1993**, *115*, 3250. (c) Roux, B.; Karplus, M. *J. Comput. Chem.* **1995**, *16*, 690.
- Sunner, J.; Kebarle, P. *J. Am. Chem. Soc.* **1984**, *106*, 6135.
- Dzidic, I.; Kebarle, P. *J. Phys. Chem.* **1970**, *74*, 1466.
- Davidson, W. R.; Kebarle, P. *J. Am. Chem. Soc.* **1976**, *98*, 6125.
- Yamashita, M.; Fenn, J. B. *J. Phys. Chem.* **1984**, *88*, 4451. Fenn, J. B.; Mann, M.; Meng, C. K.; Wong, S. F.; Whitehouse, C. M. *Science* **1985**, *246*, 64.
- (a) Jayaweera, P.; Blades, A. T.; Ikonoumou, M. G.; Kebarle, P. *J. Am. Chem. Soc.* **1990**, *112*, 2452–2454. (b) Blades, A. T.; Jayaweera, P.; Ikonoumou, M. G.; Kebarle, P. *J. Chem. Phys.* **1990**, *92*, 2900–2906. (c) Blades, A. T.; Jayaweera, P.; Ikonoumou, M. G.; Kebarle, P. *Int. J. Mass Spectrom. Ion Processes* **1990**, *102*, 251–267. (d) Blades, A. T.; Jayaweera, P.; Ikonoumou, M. G.; Kebarle, P. *Int. J. Mass Spectrom. Ion Processes* **1990**, *101*, 325–336.
- Bruins, A. P.; Covey, T. R.; Henion, J. D. *Anal. Chem.* **1987**, *59*, 2642. Covey, T. R.; Bonner, R. F.; Shushan, B. I.; Henion, J. D. *Rapid Commun. Mass Spectrom.* **1988**, *2*, 249. Huang, E. C.; Henion, J. D. *J. Am. Soc. Mass Spectrom.* **1990**, *1*, 158.
- Blades, A. T.; Kebarle, P. *J. Am. Chem. Soc.* **1994**, *116*, 10761.
- Smith, R. D.; Loo, J. A.; Edmonds, C. G.; Barinaga, C. J.; Udseth, H. R. *Anal. Chem.* **1990**, *62*, 882.
- Klassen, J.; Blades, A. T.; Kebarle, P. *J. Phys. Chem.* **1995**, *99*, 15509.
- Klobukowski, M. *Can. J. Chem.* **1992**, *70*, 589.
- Armentrout, P. B. Thermochemical Measurements by Guided Ion Beam Mass Spectrometry. In *Advances in Gas Phase Ion Chemistry*; Adams, N., Babcock, L. M., Eds.; JAI Press Inc.: Greenwich, CT, 1992; Vol. 1, p 83.
- Sunderlin, L. S.; Wang, D.; Squires, R. R. *J. Am. Chem. Soc.* **1993**, *115*, 12060. Mazinelli, P. J.; Paulino, J. A.; Sunderlin, L. S.; Wenthold, P. G.; Poutsma, J. C.; Squires, R. R. *Int. J. Mass Spectrom. Ion Processes* **1994**, *130*, 89.
- Anderson, S. G.; Blades, A. T.; Klassen, J. S.; Kebarle, P. *Int. J. Mass Spectrom. Ion Processes* **1995**, *141*, 217.
- Reid, N. M.; Buckley, J. A.; French, J. B.; Poon, C. C. *Adv. Mass Spectrom. B* **1979**, *8*, 1843.
- Dalleska, N. F.; Honma, K.; Armentrout, P. B. *J. Am. Chem. Soc.* **1993**, *115*, 12125.
- Chupka, W. A. *J. Chem. Phys.* **1959**, *30*, 191.
- Loh, S. K.; Hales, D. A.; Lian, L.; Armentrout, P. *J. Chem. Phys.* **1989**, *90*, 5466. Hales, D. A.; Lian, L.; Armentrout, P. *Int. J. Mass Spectrom. Ion Processes* **1990**, *102*, 269.
- Robinson, P. J.; Holbrook, K. A. *Unimolecular Reactions*; Wiley Interscience: New York, 1972.
- Wenthold, P. G.; Squires, R. R. *J. Am. Chem. Soc.* **1994**, *116*, 6401.
- More, M. B.; Glendening, E. D.; Ray, D.; Feller, D.; Armentrout, P. B. *J. Phys. Chem.* **1996**, *100*, 1605.
- Jensen, F. *J. Am. Chem. Soc.* **1992**, *114*, 9533.
- Taft, R. W.; Anvia, F.; Gal, J. F.; Walsh, S.; Capon, M.; Holmes, M. C.; Hosh, K.; Oloumi, G.; Vasanwala, R.; Yazdani, S. *Pure Appl. Chem.* **1990**, *62*, 17.
- The Li^+ affinity differences given in ref 29 correspond to free energy differences, i.e., changes in the $-\Delta G^\circ$, at 298 K for reaction 1.
- Bouchonnet, S.; Hoppilliard, Y. *Org. Mass Spectrom.* **1992**, *27*, 71.
- Weller, T.; Lochman, R.; Meiler, W. *J. Mol. Struct.* **1982**, *90*, 81.
- Bojesen, G.; Breindahl, T.; Andersen, U. N. *Org. Mass Spectrom.* **1993**, *28*, 1448.
- Guo, B. C.; Conklin, B. J.; Castleman, A. W., Jr. *J. Am. Chem. Soc.* **1989**, *111*, 6506.
- Arseniev, A. S.; Bystrov, V. F.; Ivanov, T. V.; Ovchinikov, Y. A. *FEBS Lett.* **1985**, *186*, 168.
- Beauchamp, J. L., private communication.